ISME

On the Co-rotational Beam Element Formulation in Large Deformation Analysis

A. Kermanian[*]
M.Sc.

A. Taghvaeipour[†]
Assistant Professor

A. Kamali[‡]
Assistant Professor

This paper sheds more light on the co-rotational element formulation for beams with uniform cross-section. The co-rotational elements are commonly used in problems in which a structure undergoes a large deformation. In this study, the foregoing element obeys the Euler-Bernoulli beam assumptions. Unlike the formulations presented in the literature, in this paper, a number of local nodal coordinates are employed which makes the kinematic description of the deformed beam much easier without the need of expressing any complicated relations. In this regard, via a case study, the methodology is implemented step-by-step, and the results are compared with the ones calculated analytically and by means of elliptic integrals. The methodology is briefly formulized for 3D cases as well.

Keywords: Large deformation, Co-rotational Element Formulation, Euler-Bernoulli beam theory, Elliptic integrals

1 Introduction

Mechanical analysis of flexible parts is a complicated task in the embodiment design stage of machinery and structures. Although, in many cases, the parts can be assumed to be rigid, there exist situations in which the flexibility comes to an effect in the form of unwanted vibrations and large deformation of the parts. For example, when a mechanism is designed to carry a heavy load or to act very fast and accurate, the rigidity is a wrong assumption and the flexibility of the components must be taken into account.

In mechanical systems such as mechanisms and manipulators, there are flexible components which can be modelled based on the beam theory. Due to the geometry and loading conditions, beam-like flexible components can undergo large deformations. This phenomenon can significantly affect the kinematic accuracy and reliability of a mechanism or manipulator, especially in pick-and-place operations where the kinematic accuracy is very crucial.

[*]M.Sc., Mechanical Engineering Department, Amirkabir University of Technology (Tehran Polytechnic), Tehran, alikermanian@aut.ac.ir

[†]Corresponding Author, Assistant Professor, Mechanical Engineering Department, Amirkabir University of Technology (Tehran Polytechnic), Tehran, ataghvaei@aut.ac.ir

[‡]Assistant Professor, Mechanical Engineering Department, Amirkabir University of Technology (Tehran Polytechnic), Tehran, alikamalie@aut.ac.ir

Therefore, static and dynamic analyses of mechanical system should be conducted while the flexible beam-like components are modelled under the large deformation assumption. There is a vast amount of literature on the large deformation of beams, and various approaches have been proposed. In the sequel, a couple of common methodologies are reviewed.

A common approach to solve a large deformation problem of a beam analytically is to incorporate elliptic integrals. Bisshopp and Drucker [1] used the Euler-Bernoulli beam theory, taking to the account the square of slope in the curvature formula, and obtained a complicated differential equation. Then, by resorting to the elliptic integrals the differential equations were solved. Detailed information of the corresponding closed-form solution can be found in [2]. Zhang and Chen also presented a more general elliptic integral solution for large deformation problems [3]. Computing the elliptic integrals offers the most accurate solution for thin beams undergoing large deformation; hence, it can be used as a criterion to evaluate other numerical methods. However, the calculation of the elliptic integrals itself is quite complicated.
Instead of dealing with elliptic integrals, Wang and Kitipornchai used a mixed optimization and shooting method to solve the nonlinear differential equation of a large deformation problem [4]. Also Pai and Palazotto used a multiple shooting method to gain the large deflection of curved beams [5]. Yin et al. offered a number of computational models to deal with a large deformation of flexible fingers. By computing an effective flexural rigidity (EI) numerically, they could provide a uniform approximate model of non-uniform fingers [6].

The finite element method (FEM) is a common numerical approach that is extensively used in the nonlinear analysis of structures. In this case, different methods have been developed to cope with issues such as geometric nonlinearities, material nonlinearities, large deformations, large strains, and etc. Bathe et al. [7] presented a comprehensive review on this matter and implemented a detailed derivation and comparison of general nonlinear finite element formulations based on continuum mechanics. Also, Bathe and Bolourchi presented an updated lagrangian and a total lagrangian formulation for a 3D beam element and compared the two methods in terms of computational efficiency and effectiveness [8]. In [9], Pai et al. presented a total lagrangian displacement based on finite element formulation for general beams. The authors also compared the experimental and the numerical results. Borri and Merlini proposed a formulation for the large deformation of inhomogeneous beams [10].

In addition to the total lagrangian and the updated lagrangian, the co-rotational (CR) finite element formulation is another tool to deal with geometric nonlinearities. The CR description is based on the polar decomposition theory in which the deformation of a body is splitted into two components, rigid motion and relative deformation. This method simplifies the derivation of the lagrangian formulations for large deflection problems, however, it suffers from a kinematic limitation: the displacements or rotations can be large but the deformations must remain small. A number of planar cases have been investigated in [11] and a comprehensive review on this subject is presented in [12].

The absolute nodal coordinates is another method which is very suitable for the simulation of flexible multibody systems. In this method, a set of coordinates such as absolute nodal displacements, absolute nodal slopes, and etc. are defined in the inertia frame which results in a constant mass matrix and a highly nonlinear stiffness matrix [13]. This method does not need any incremental procedure which is very advantageous, details can be obtained in [14,15]. By considering the shear effects as well, an absolute nodal coordinate formulation was presented for 3D beam elements in [16]. Gerstmayr et al. [17] presented a comprehensive review on this subject.
This paper sheds more light on the CR formulation of a planar Euler-Bernoulli beam while it undergoes large deformation. Accordingly, the large deformation of the beams with uniform cross-section is obtained by incorporating a straight-forward and non-iterative algorithm.

According to the co-rotational formulations presented in the literature, the co-rotated rigid axis of each element is usually chosen to be the connecting line of the end nodes; also, the nodal coordinates are described in a fixed global reference frame. In this study however, the co-rotated rigid axis of the element is chosen to be always tangent to centroid curve of the deformed element at the first node, therefore, each element can be considered as a cantilever beam in its co-rotated frame. Also, instead of using global nodal coordinates, a set of local nodal coordinates are employed for each element, which makes the kinematic description of the deformed beam much more easier without the need of expressing any complicated relations.

In this regard, first, the CR formulation is comprehensively explained by simple words. Next, the method is illustrated by implementing on a simple planar cantilever beam, and the necessary equations are derived. Then, the numerical results are compared with the closed form solution obtained by the elliptic integrals presented in [1-3]. Afterwards, a general formulation to solve the planar and spatial cantilever beams undergoing large deformation is presented. In the next step, a discussion is conducted regarding the accuracy of the proposed formulation. Also, the foretold formulation is also implemented on a planar beam with simple- simple boundary conditions at the end points and the numerical results are validated by the use of the commercial software MSC. ADAMS. Finally, the overall results are discussed.

2 The CR Beam Formulation for a Planar Beam

In the Euler-Bernoulli beam theory the bending moment is related to the curvature proportionally, namely,

$$M = EI\frac{d\theta}{ds} = EI\frac{\frac{d^2y}{dx^2}}{\left(1+\left(\frac{dy}{dx}\right)^2\right)^{\frac{3}{2}}} \tag{1}$$

If the small deformation assumption is made, then it yields

$$\left(\frac{dy}{dx}\right)^2 \approx 0 \tag{2}$$

And the Eq. (1) is linearized as below,

$$M = EI\frac{d^2y}{dx^2} \tag{3}$$

However, for a cantilever beam which undergoes a large deformation (Figure (1)) the assumption in Eq. (2) cannot be considered.

Apparently, the angle of slope which is measured from the horizontal X axis increases nonlinearly from the base toward the end point. Hence, the assumption in Eq. (2) is no more valid. Now, the nodes N_1 to N_4 are selected on the central axis of the beam (depicted in Figure (1)). It is obvious that

$$\delta\theta_4 > \delta\theta_3 > \delta\theta_2 > \delta\theta_1 > 0$$

where $\delta\theta_i$ is the angle of slope at the node N_i. Because of the large deformation it yields that

$$\left.\frac{dy}{dx}\right|_{N_i} = \tan(\delta\theta_i) \neq 0 \quad , \quad i = 1,2\ldots4 \tag{4}$$

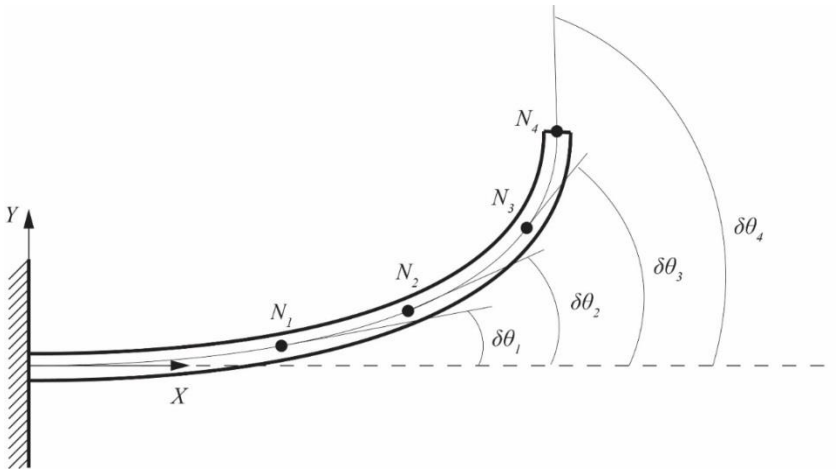

Figure 1 A large deflected cantilever beam

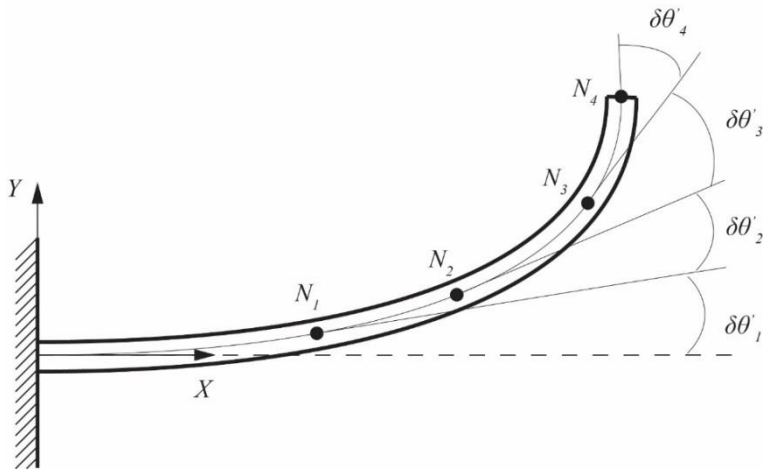

Figure 2 Relative angles of slopes

Now, the angle of slope at N_i relative to the angle of slope at N_{i-1} is denoted by $\delta\theta_i^{'}$ and depicted in Figure (2). According to Figure (1) and Figure (2), it is obvious that:

$$\delta\theta_i^{'} < \delta\theta_i \quad i = 2,3,4$$

This expresses that by dividing a beam into a number of elements, the relative deflection of each node with respect to the previous one is smaller than its absolute deflection. Hence, with a proper discretization, it can be assumed that each element undergoes small deformation, and as a result, the classic Euler-Bernoulli beam equation (Eq. (3)) can be applied for each element. In other words, a flexible beam-like component which undergoes a large deformation is discretized into some beam elements with the small deformation assumption. In the sequel, the method is illustrated in detail.

3 Case Study

In this section, without loss of generality, the CR beam element is explained via its implementation on a case study. The case study is a simple planar cantilever beam which is loaded by an external vertical force P as shown in Figure (3).

In this case, it is assumed that the beam undergoes large deformation after applying the external load P. Hence, the beam is first divided into number of elements, here three elements

is used. Next, a moving coordinate reference frame, namely, the co-rotated frame, is attached to each node.

Note that the origin of each local coordinate frame (X_i, Y_i, Z_i) is placed on the respective node (i) so as the axis X_i is tangent to the curve of the central axis of the deformed beam. These details are illustrated in Figure (4).

As the case study is planar, three deformation variables δx, δy and δθ are introduced for each node. δx_i, δy_i and $\delta\theta_i$ are the displacement of the (i)th node with respect to (i-1)th node along the axis x_{i-1}, along the axis y_{i-1} and the angle of rotation of the (i)th node with respect to the (i-1)th node messured about the axis z_{i-1}, respectively.

The rotation matrix from (i-1)th frame to (i)th frame is defined as:

$$ {}^{i}_{i-1}\mathbf{R} = \begin{bmatrix} \cos\ \delta\theta_i & \sin\ \delta\theta_i \\ -\sin\ \delta\theta_i & \cos\ \delta\theta_i \end{bmatrix} \tag{5} $$

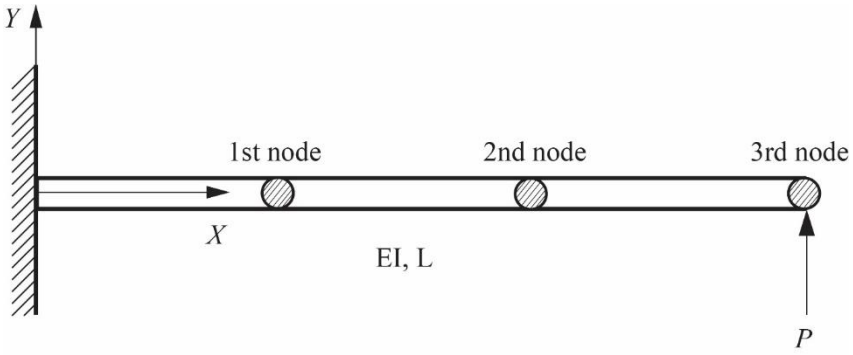

Figure 3 A simple cantilever beam before deformation

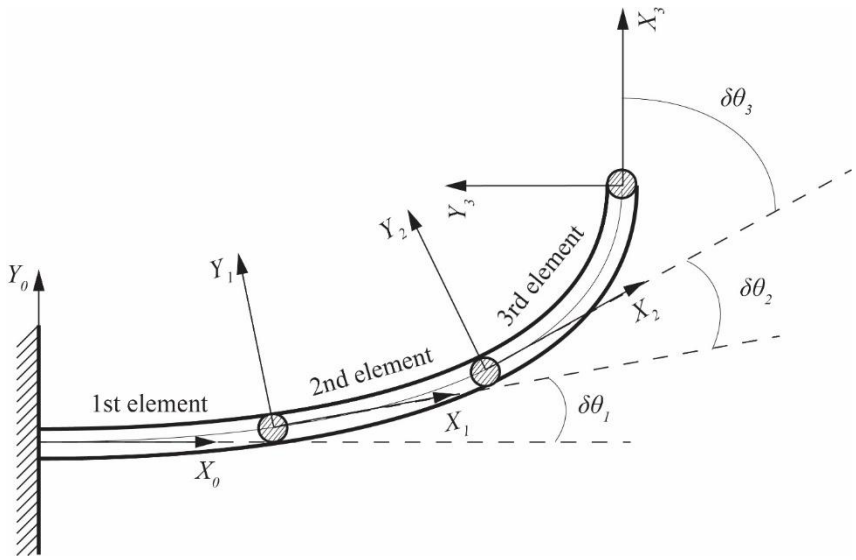

Figure 4 The cantilever beam after deformation

By considering each element as a simple cantilever beam with respect to the previous element and using the Euler-Bernoulli beam theory, the stiffness matrix of the (i)th element in the (i-1)th frame is [19]:

$$\mathbf{K_i} = \begin{bmatrix} \frac{E_i A_i}{l_i} & 0 & 0 \\ 0 & \frac{12E_i I_i}{l_i^3} & -\frac{6E_i I_i}{l_i^2} \\ 0 & -\frac{6E_i I_i}{l_i^2} & \frac{4E_i I_i}{l_i} \end{bmatrix} \tag{6}$$

The nodal force vector of the (i)th node is denoted by:

$$\mathbf{f_i} = [f_{ix} \quad f_{iy}]^T \tag{7}$$

and the (3×1) nodal load vector which contains the planar forces and the bending torque at the (i)th node expressed in the (i-1)th frame is defined as below:

$$\mathbf{W_i} = [f_i \quad m_{iz}]^T \tag{8}$$

and the planar deformation vector of the (i)th node in the (i-1)th frame is:

$$\mathbf{\Delta_i} = [\delta x_i \quad \delta y_i \quad \delta\theta_i]^T \tag{9}$$

As it was mentioned before, to solve a large deformation problem, it is assumed that each element is a cantilever beam, this means that the (i)th element is a simple cantilever beam whose base is attached to the end of the (i-1)th element.

These details are illustrated in Figure (5).

Now, the deformation and the load vectors of the (i)th element, expressed in the (i-1)th frame, is related via matrix $\mathbf{K_i}$:

$$\mathbf{W_i = K_i \Delta_i} \tag{10}$$

According to Eq. (5), the transformation matrices between the frames are:

$${}^{1}_{0}\mathbf{R} = \begin{bmatrix} \cos\ \delta\theta_1 & \sin\ \delta\theta_1 \\ -\sin\ \delta\theta_1 & \cos\ \delta\theta_1 \end{bmatrix} \tag{11}$$

$${}^{2}_{1}\mathbf{R} = \begin{bmatrix} \cos\ \delta\theta_2 & \sin\delta\theta_2 \\ -\sin\ \delta\theta_2 & \cos\ \delta\theta_2 \end{bmatrix} \tag{12}$$

Therefore, the external force vector on the third node in the second frame is calculated as

$$\mathbf{f_3} = \begin{Bmatrix} f_{3x} \\ f_{3y} \end{Bmatrix} = \left[{}^{2}_{1}\mathbf{R}\right]\left[{}^{1}_{0}\mathbf{R}\right]\mathbf{P}_{load} = \begin{bmatrix} \cos\ \delta\theta_2 & \sin\delta\theta_2 \\ -\sin\ \delta\theta_2 & \cos\ \delta\theta_2 \end{bmatrix} \times \begin{bmatrix} \cos\ \delta\theta_1 & \sin\ \delta\theta_1 \\ -\sin\ \delta\theta_1 & \cos\ \delta\theta_1 \end{bmatrix} \begin{Bmatrix} 0 \\ P \end{Bmatrix} = \begin{Bmatrix} P\sin(\delta\theta_1+\delta\theta_2) \\ P\cos(\delta\theta_1+\delta\theta_2) \end{Bmatrix} \tag{15}$$

in which

$$\mathbf{P_{load}} = [0 \quad P]^T \tag{13}$$

and the torque on this node is zero, namely,

$$M_3 = M_{3z} = 0 \tag{14}$$

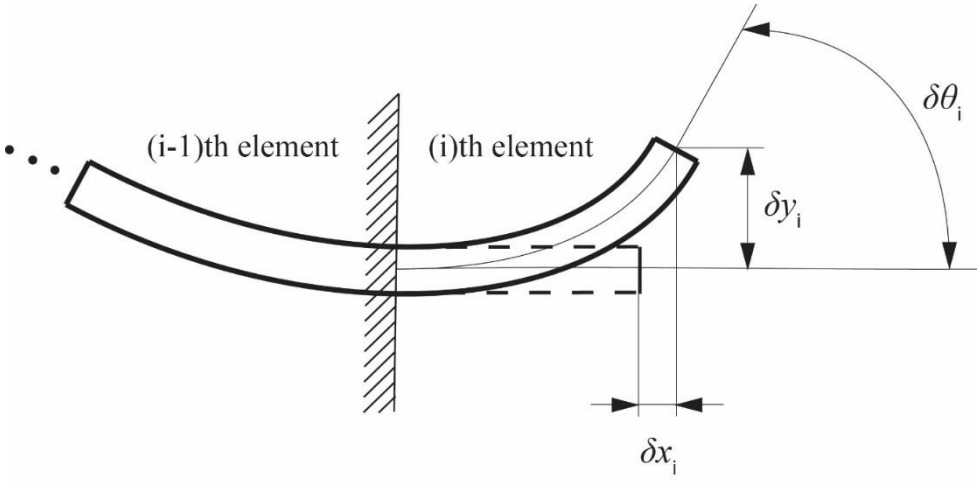

Figure 5 Deformation of an element with respect to previous one

Hence, the planar wrench array on this node becomes

$$\mathbf{W_3} = \begin{Bmatrix} f_{3x} \\ f_{3y} \\ M_{3z} \end{Bmatrix} = \begin{bmatrix} P\sin(\delta\theta_1+\delta\theta_2) \\ P\cos(\delta\theta_1+\delta\theta_2) \\ 0 \end{bmatrix} \tag{16}$$

The equilibrium equation for the third element in the second frame is:

$$\mathbf{W_3} = \mathbf{K_3}\boldsymbol{\Delta_3} \tag{17}$$

Now the first set of key equations is obtained as below,

$$\boldsymbol{\Delta_3} = \begin{Bmatrix} \delta x_3 \\ \delta y_3 \\ \delta\theta_3 \end{Bmatrix} = \mathbf{K_3}^{-1}\mathbf{W_3} \tag{18}$$

By expanding the Eq. (18) it yields:

$$\delta x_3 = \frac{Pl_e\sin(\delta\theta_1+\delta\theta_2)}{AE} \tag{19}$$

$$\delta y_3 = \frac{Pl_e^3\cos(\delta\theta_1+\delta\theta_2)}{3EI} \tag{20}$$

$$\delta\theta_3 = \frac{Pl_e^2\cos(\delta\theta_1+\delta\theta_2)}{2EI} \tag{21}$$

In the next step, the equilibrium equation of the second element is expressed in the first frame; as before, the force on the second node is

$$\mathbf{f_2} = \left[{}^1_0\mathbf{R}\right]\mathbf{P}_{load} = \begin{bmatrix} \cos\delta\theta_1 & \sin\delta\theta_1 \\ -\sin\delta\theta_1 & \cos\delta\theta_1 \end{bmatrix}\begin{Bmatrix} 0 \\ P \end{Bmatrix} = \begin{Bmatrix} P\sin(\delta\theta_1) \\ P\cos(\delta\theta_1) \end{Bmatrix} \tag{22}$$

After the deformation, the position vector of the third node in the second frame equals

$$\mathbf{r_3} = [l_e+\delta x_3 \quad \delta y_3]^T \tag{23}$$

Also, the torque on the second node is obtained as following

$$M_2 = M_{z2} = \mathbf{r}_3\times\mathbf{f}_3+\mathbf{m}_{3z} = [P(l_e+\delta x_3)\cos(\delta\theta_1+\delta\theta_2) - P\delta y_3\times\sin(\delta\theta_1+\delta\theta_2)]e_{z2} \tag{24}$$

And the planar load vector for the second node is presented as

$$\mathbf{W_2} = [\mathbf{f}_2^T \quad m_{2z}]^T \tag{25}$$

From the equilibrium of the second element, also, the following key equations are obtained,

$$\mathbf{\Delta_2}=\begin{Bmatrix}\delta x_2\\ \delta y_2\\ \delta\theta_2\end{Bmatrix}=\mathbf{K_2}^{-1}\mathbf{W_2} \tag{26}$$

After the expansion of the Eq. (26), it yields

$$\delta x_2=\frac{Pl_e\sin(\delta\theta_1)}{EA} \tag{27}$$

$$\delta y_2=\frac{Pl_e^2}{6EI}\left(3(l_e+\delta x_3)\cos(\delta\theta_1+\delta\theta_2)-3\delta y_3\sin(\delta\theta_1+\delta\theta_2)+2l_e\cos(\delta\theta_1)\right) \tag{28}$$

$$\delta\theta_2=\frac{Pl_e}{2EI}\left(2(l_e+\delta x_3)\cos(\delta\theta_1+\delta\theta_2)-2\delta y_3\sin(\delta\theta_1+\delta\theta_2)+l_e\cos(\delta\theta_1)\right) \tag{29}$$

For the first element, the external force vector, the position vector of the second node and the moment about the Z_1-axis in the global reference frame are presented below,

$$\mathbf{f_1}=[0\quad P]^T \tag{30}$$

$$\mathbf{r_2}=[l_e+\delta x_2\quad \delta y_2\ ]^T \tag{31}$$

$$M_1=M_{1z}=\{\mathbf{r_2}\}\times\{\mathbf{f_2}\}+M_2=P(l_e+\delta x_3)\cos(\delta\theta_1+\delta\theta_2)+P(l_e+\delta x_2)\cos(\delta\theta_1)-P\delta y_2\sin(\delta\theta_1)-P\delta y_3\sin(\delta\theta_1+\delta\theta_2) \tag{32}$$

and from the equilibrium equation of the first element, the last set of key equations is obtained as following

$$\mathbf{\Delta_1}=\begin{Bmatrix}\delta x_1\\ \delta y_1\\ \delta\theta_1\end{Bmatrix}=\mathbf{K_1}^{-1}\mathbf{W_1} \tag{33}$$

which results in

$$\delta x_1=0 \tag{34}$$

$$\delta y_1=\frac{Pl_e^2}{6EI}\left(l_e+2(l_e+\delta x_3)\cos(\delta\theta_1+\delta\theta_2)-2\delta y_3\sin(\delta\theta_1+\delta\theta_2)\right)+\frac{Pl_e^2}{6EI}\left(3(l_e+\delta x_2)\cos(\delta\theta_1)-3\delta y_2\sin(\delta\theta_1)\right) \tag{35}$$

$$\delta\theta_1=\frac{Pl_e}{2EI}\left(l_e+2(l_e+\delta x_3)\cos(\delta\theta_1+\delta\theta_2)-2\delta y_3\sin(\delta\theta_1+\delta\theta_2)\right)+\frac{Pl_e}{2EI}\left(2(l_e+\delta x_2)\cos(\delta\theta_1)-2\delta y_2\sin(\delta\theta_1)\right) \tag{36}$$

Eq. (19)- (21), Eq. (27)-(29) and Eq. (34)-(36) form a system of 9 nonlinear equations with 9 deformation variables. This set of nonlinear equations can be solved by resorting to numerical methods. In this study, the system of nonlinear equations is solved using Matlab fsolve function in collaboration with Trust- Region- Dogleg algorithm. The details on this algorithm can be found in [19].

At the end, the position vector of the end point can be obtained as

$$\mathbf{r_{end}}=[X\quad Y]^T=\mathbf{r}_1+\left[{}^1_0\mathbf{R}^T\right]\{\mathbf{r_2}\}+\left[{}^1_0\mathbf{R}^T\right]\left[{}^2_1\mathbf{R}^T\right]\{\mathbf{r_3}\} \tag{37}$$

$$\mathbf{r_1}=[l_e+\delta x_1\quad \delta y_1\ ]^T \tag{38}$$

From hereafter, the proposed formulation is going to be referred as CBEM (Cantilever Beam Element Method).

4 Results

In this section, the results obtained from the CBEM is compared with the closed form solution of elliptic integrals, presented in [1-3], for different load magnitudes. Let us denote the deflection of the end point calculated by elliptic integrals as,

$$\boldsymbol{\Delta}^{*}_{\mathbf{end}} = [\Delta X^{*} \quad \Delta Y^{*}] \tag{39}$$

and the deflection computed by CBEM elements as,

$$\boldsymbol{\Delta}_{\mathbf{end}} = [\Delta X \quad \Delta Y]^{T} = \mathbf{r}_{\mathbf{end}} - [L \quad 0]^{T} \tag{40}$$

The absolute error is calculated via the following formulation,

$$\mathbf{e} = \left\| \boldsymbol{\Delta}^{*}_{\mathbf{end}} - \boldsymbol{\Delta}_{\mathbf{end}} \right\| \tag{41}$$

And the relative error as,

$$\mathbf{e}^{*} = \frac{\left\| \boldsymbol{\Delta}^{*}_{\mathbf{end}} - \boldsymbol{\Delta}_{\mathbf{end}} \right\|}{\left\| \boldsymbol{\Delta}^{*}_{\mathbf{end}} \right\|} \tag{42}$$

Now, consider a simple cantilever beam as shown in Figure (3) with the length of L=250 mm, height of h=2 mm, depth of b=5 mm and Young modulus of E=170 GPa. The beam is divided into three uniform elements and a non-follower vertical force is applied on the end point. The vertical force varies from 0.5 N to 7 N.

In Figure (6), the location of the end point after deformation is shown for each load due to the results of CBEM, Elliptic integrals and also the classic Euler-Bernouli small deformation formulation. The absolute and relative errors are shown in Figure (7) and (8) for each load magnitude.

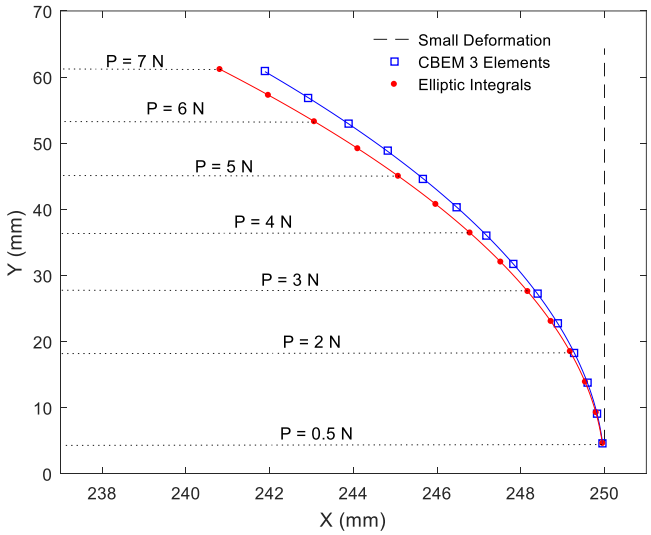

Figure 6 Location of the end point after deformation

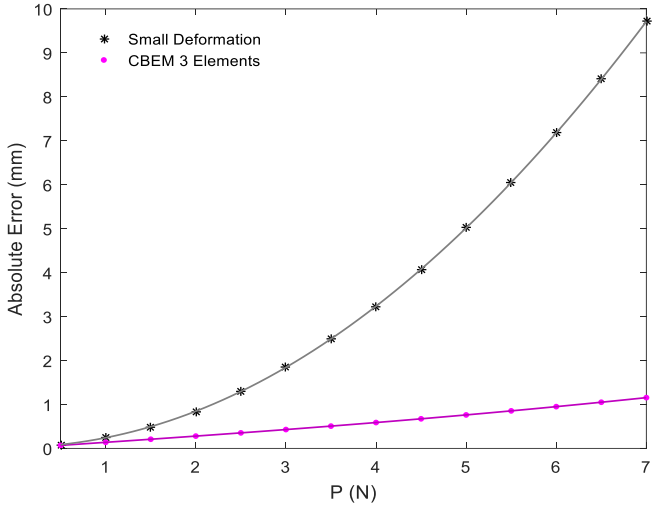

Figure 7 Plot of Absolute Error

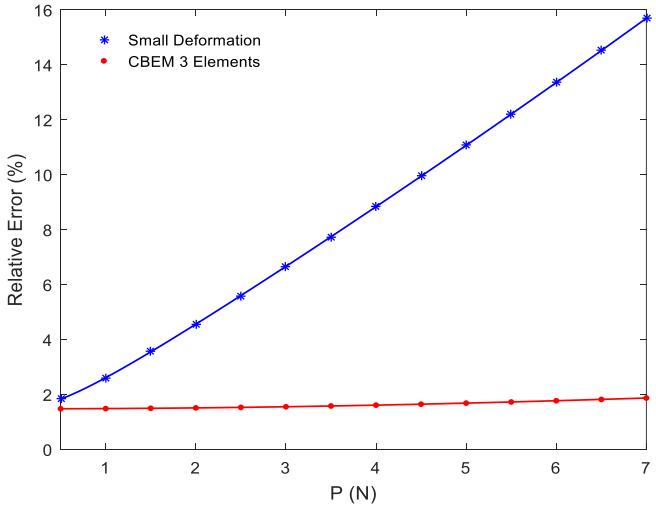

Figure 8 Plot of Relative Error

5 A General Algorithm for Large Deformation Analysis of a Planar Cantilever Beam

Here, a general algorithm for the static analysis of a planar cantilever beam undergoing a large deformation is presented. First of all, the following assumptions are taken into consideration:

1. The beam is divided into (n) elements, and the cross section area of each element is uniform along the element.
2. Each element is considered as an Euler – Bernoulli cantilever beam with respect to prior element.
3. The external load is applied at the end point of the beam.
4. The material is linear elastic.

The procedure contains the following steps:

Step 1:

Obtain the transformation matrix between each adjacent frame. The transform matrix from the (i)th frame to the (i-1)th frame is

$$ {}^{i}_{i-1}\mathbf{R} = \begin{bmatrix} \cos\ \delta\theta_i & \sin\ \delta\theta_i \\ -\sin\ \delta\theta_i & \cos\ \delta\theta_i \end{bmatrix} \tag{43} $$

Step 2:

Find the load vector on the (i)th node with respect to the (i-1)th frame. The applied external force is

$$\mathbf{f_{ext}} = [P_x \quad P_y]^T \tag{44}$$

and the external torque equals

$$\mathbf{M_{ext}} = m_{ext_z}\, \mathbf{e}_z \tag{45}$$

Then, the force vector on the (i)th node with respect to the (i-1)th frame is defined as following

$$\mathbf{f_1} = \mathbf{f_{ext}} \tag{46}$$

$$\mathbf{f_i} = \left(\prod_{k=1}^{i-1} {}^{k}_{k-1}\mathbf{R} \right) \mathbf{f_{ext}} \quad , \quad i \neq 1 \tag{47}$$

The position vector of the (i)th node in the (i-1)th frame is defined as

$$\mathbf{r_i} = [l_e + \delta x_i \quad \delta y_i]^T \tag{48}$$

Also, the torque applied on the (i)th node is calculated as

$$\mathbf{M_i} = m_{iz} = \{M_{i+1}\} + \{\mathbf{r_i}\} \times \{\mathbf{f_i}\} \ , \ i \neq n \tag{49}$$

$$\mathbf{M_n} = \mathbf{M_{ext}} \tag{50}$$

Finally, the load vector on the (i)th node in the (i-1)th frame is cast in the following form,

$$\mathbf{W_i} = [f_i \quad m_{iz}]^T \tag{51}$$

Step 3:

By considering each element as a cantilever beam, the equilibrium equation can be presented

$$\mathbf{W_i} = \mathbf{K_i} \Delta_i \tag{52}$$

In which Δ_i is the deformation vector of the (i)th node in the (i-1)th frame, namely,

$$\Delta_i = [\delta x_i \quad \delta y_i \quad \delta \theta_i]^T \tag{53}$$

and $\mathbf{K}_i$ is the stiffness matrix, and for a planar cantilever beam element it is obtained as [18]

$$\mathbf{K_i} = \begin{bmatrix} \frac{EA}{l_e} & 0 & 0 \\ 0 & \frac{12EI}{l_e^3} & -\frac{6EI}{l_e^2} \\ 0 & -\frac{6EI}{l_e^2} & \frac{4EI}{l_e} \end{bmatrix} \tag{54}$$

Then, the set of key equations for the (i)th element can be derived as:

$$\Delta_i = \mathbf{K_i^{-1}} \mathbf{W_i} \tag{55}$$

As a result, a system of 3n nonlinear equations with 3n deformation unknowns is obtained. These equations are solved numerically which provides the deformation at any point of the beam.

6 General Algorithm for Large Deformation Analysis of a Spatial Cantilever Beam

In this section we are going to introduce a straight forward mathematical procedure to solve the spatial large deformation of a cantilever beam under an external load at the end. The steps and the assumptions in this case are very similar to the planar case.

First, a vector for the nodal relative displacements is defined as below,

$$\Delta_{\mathbf{i}} = [\delta x_i \quad \delta y_i \quad \delta z_i \quad \delta\theta_{ix} \quad \delta\theta_{iy} \quad \delta\theta_{iz}]^T$$

Then, the key equations are governed similar to what was presented for a planar case.

In the 3D space, the transform matrix from (i)th frame to the (i-1)th frame is

$$\mathbf{{}^{i}_{i-1}R} = \begin{bmatrix} \cos\delta\theta_{iz} & \sin\delta\theta_{iz} & 0 \\ -\sin\delta\theta_{iz} & \cos\delta\theta_{iz} & 0 \\ 0 & 0 & 1 \end{bmatrix} \times \begin{bmatrix} \cos\delta\theta_{iy} & 0 & -\sin\delta\theta_{iy} \\ 0 & 1 & 0 \\ \sin\delta\theta_{iy} & 0 & \cos\delta\theta_{iy} \end{bmatrix} \times \begin{bmatrix} 1 & 0 & 0 \\ 0 & \cos\delta\theta_{ix} & \sin\delta\theta_{i} \\ 0 & -\sin\delta\theta_{ix} & \cos\delta\theta_{ix} \end{bmatrix} \quad (56)$$

The applied external force and torque are

$$\mathbf{f_{ext}} = [P_x \quad P_y \quad P_z]^T \quad (57)$$

$$\mathbf{M_{ext}} = [M_x \quad M_y \quad M_z]^T \quad (58)$$

Accordingly, the external wrench array is defined as,

$$\mathbf{W_{ext}} = [\mathbf{f_{ext}^T} \quad \mathbf{M_{ext}^T}]^T \quad (59)$$

The nodal forces are also can be presented as,

$$\mathbf{F_1} = \mathbf{F_{ext}}$$

$$\mathbf{F_i} = \left(\prod_{k=1}^{i-1} \mathbf{{}^{k}_{k-1}R} \right) \mathbf{F_{ext}} \quad , \quad i \neq 1 \quad (60)$$

Moreover, the position vector of the (i)th node in the (i-1)th frame is

$$\mathbf{r_i} = [l_e + \delta x_i \quad \delta y_i \quad \delta z_i]^T \quad (61)$$

The nodal torque vectors and the corresponding wrench array are defined as,

$$\mathbf{M_n} = \mathbf{M_{ext}}$$

$$\mathbf{M_i} = \left(\prod_{k=1}^{i-1} \mathbf{{}^{k}_{k-1}R} \right) \mathbf{M_{i+1}} + \{\mathbf{r_i}\} \times \{\mathbf{F_i}\} \quad , \quad i \neq n \quad (62)$$

$$\mathbf{W_i} = [\mathbf{F_i^T} \quad \mathbf{M_i^T}]^T$$

The stiffness matrix of a 3D cantilever beam element can be presented below

$$\mathbf{K_i} = \begin{bmatrix} \frac{EA}{l_e} & 0 & 0 & 0 & 0 & 0 \\ 0 & \frac{12EI_z}{l_e^3} & 0 & 0 & 0 & -\frac{6EI_z}{l_e^2} \\ 0 & 0 & \frac{12EI_y}{l_e^3} & 0 & \frac{6EI_y}{l_e^2} & 0 \\ 0 & 0 & 0 & \frac{G_eI_{ex}}{l_e} & 0 & 0 \\ 0 & 0 & \frac{6EI_y}{l_e^2} & 0 & \frac{4EI_y}{l_e} & 0 \\ 0 & -\frac{6EI_z}{l_e^2} & 0 & 0 & 0 & \frac{4EI_z}{l_e} \end{bmatrix} \quad (63)$$

Finally, the set of key equations for each element in a large deformation problem can be derived as,

$$\Delta_i = \mathbf{K_i}^{-1}\mathbf{W_i} \tag{64}$$

At the end, a system of $(6n)$ nonlinear equations of $(6n)$ deformation variables is obtained.

7 The accuracy of CBEM

As it was mentioned before, the displacement of each node relative to the previous node is smaller than its absolute displacement which permits the use of the linear Euler-Bernoulli beam equation for each element. However, if the beam component is divided into more number of elements, the relative nodal deflections become much smaller, and as a result, the accuracy of CBEM gets even higher. In this section, the effect of number of elements on the accuracy of CBEM is investigated.

Here, the accuracy of CBEM is tested via the beam that was introduced in section (4) and under the same load case. By using the results of elliptic integrals as a criterion, the location of the end point, after a large deformation, is shown in Figure (9) for different number of elements. The relative and absolute errors are shown in Figure (10) and (11).

As Figure (9) depicts, the curve obtained by CBEM becomes closer to the elliptic integrals curve as the number elements increases. According to Figure (10) and (11), by increasing the number of elements, the CBEM can solve the problem more accurate; however, it has a limit. It is seen that when the number of elements increases from 6 to 8, the CBEM results and the associated errors do not change significantly.

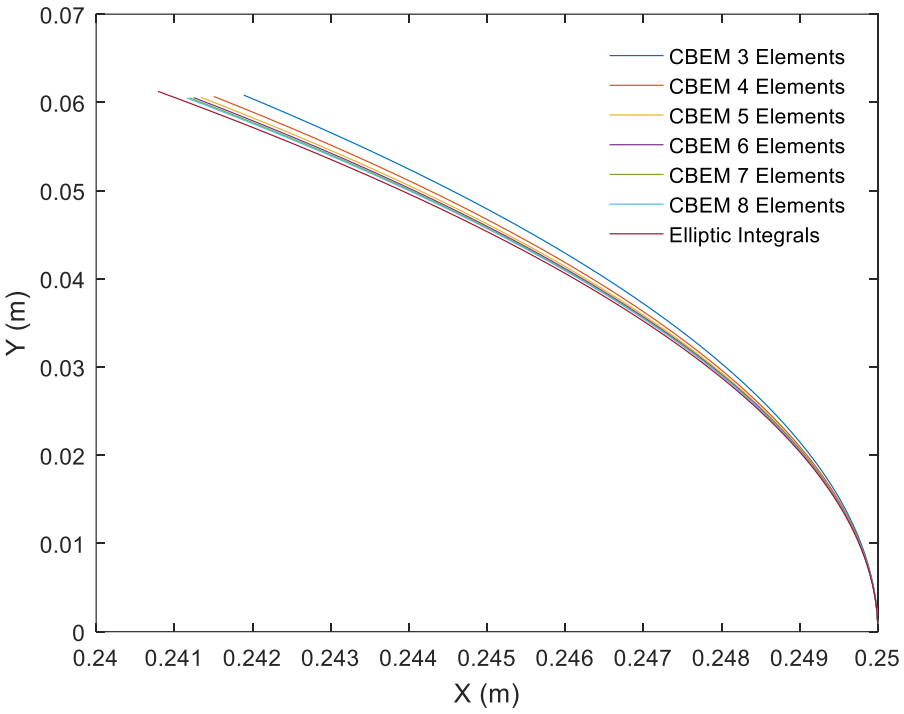

Figure 9 Location of the end point using different numbers of elements

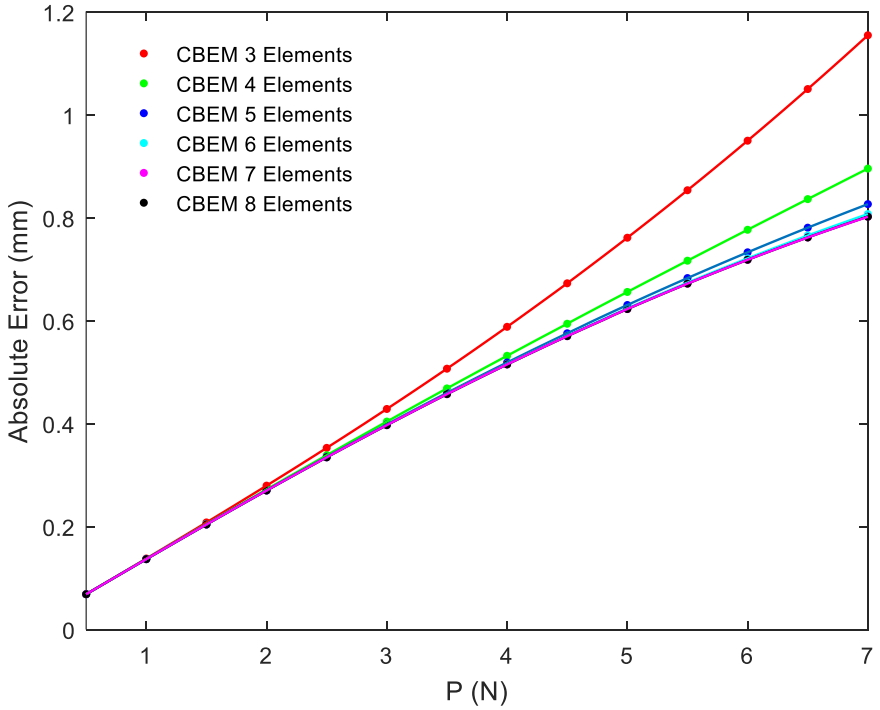

Figure 10 Absolute error of CBEM for different numbers of elements and load magnitudes

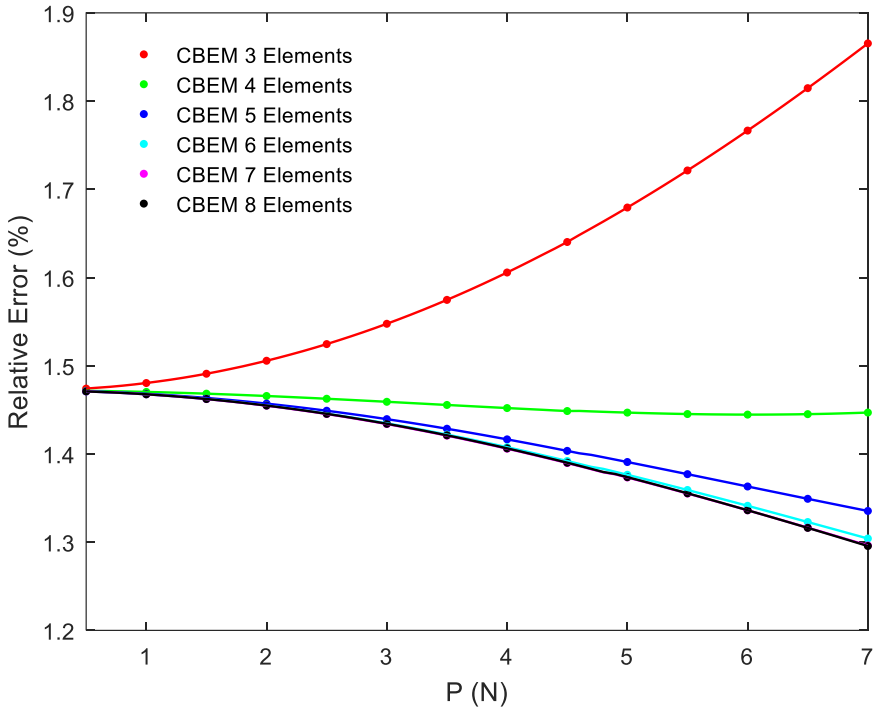

Figure 11 Relative error of CBEM for different numbers of elements and load magnitudes

8 Implementation on a planar beam with simple-simple boundary conditions

Figure (12) shows a beam which has simple-simple boundary conditions at the end points. A fixed reference frame (X, Y, Z) is located at point *A*. The beam is under a vertical force F along the opposite direction of Y-axis, at the midpoint.

Also the right hand end point of the beam (B) is allowed to move along X-axis. The mathematical procedure is elaborated in the Appendix.

The beam has the length of 100 cm, uniform cross section of 0.4×2 cm^2 and Young modulus of 71.705 GPa. By using 20 elements, CBEM is implemented for different load magnitudes. Also, in order to validate the numerical results, this beam is modeled in MSC. Adams. Figure (13), depicts the position of the midpoint after the deformation. Figure (14) shows the deformed beam.

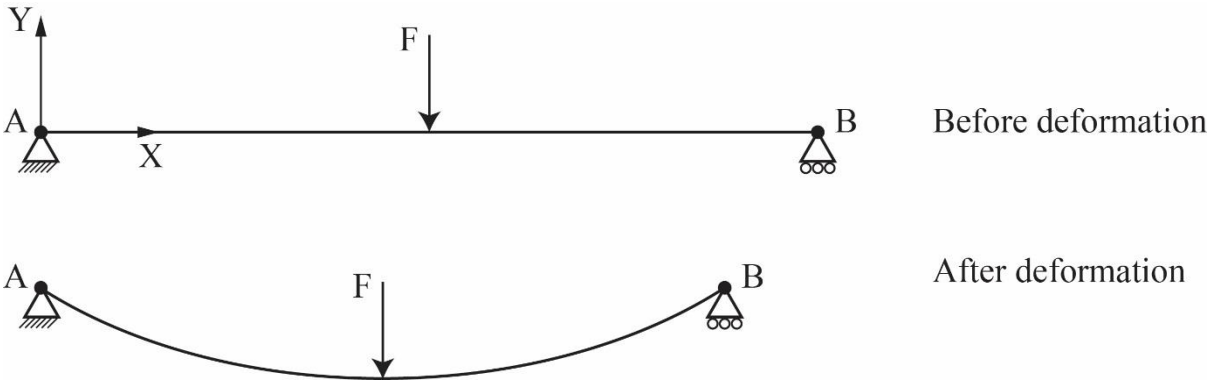

Figure 12 The planar beam with simple- simple boundary conditions

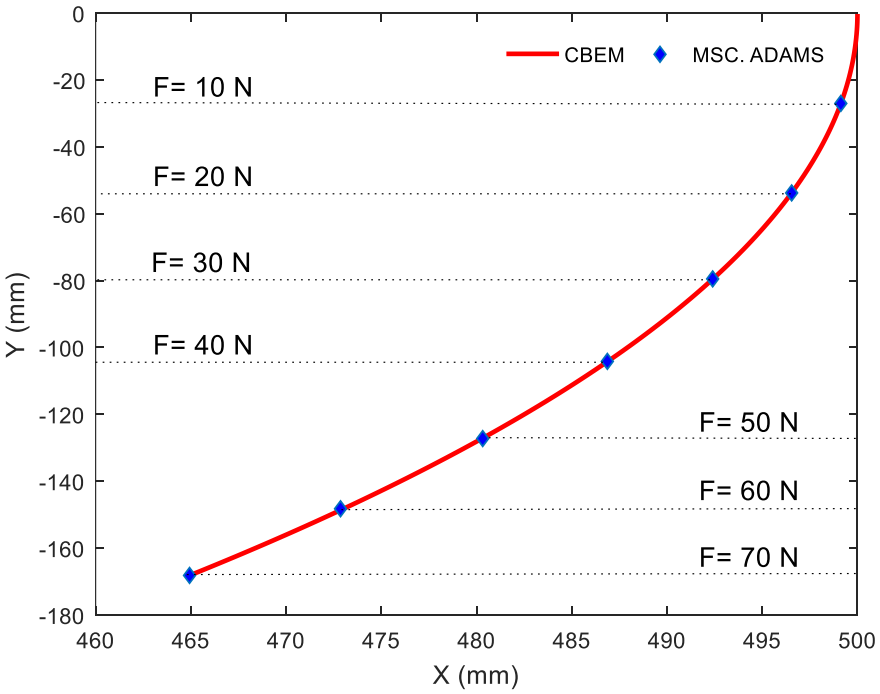

Figure 13 The position of the midpoint after the deformation

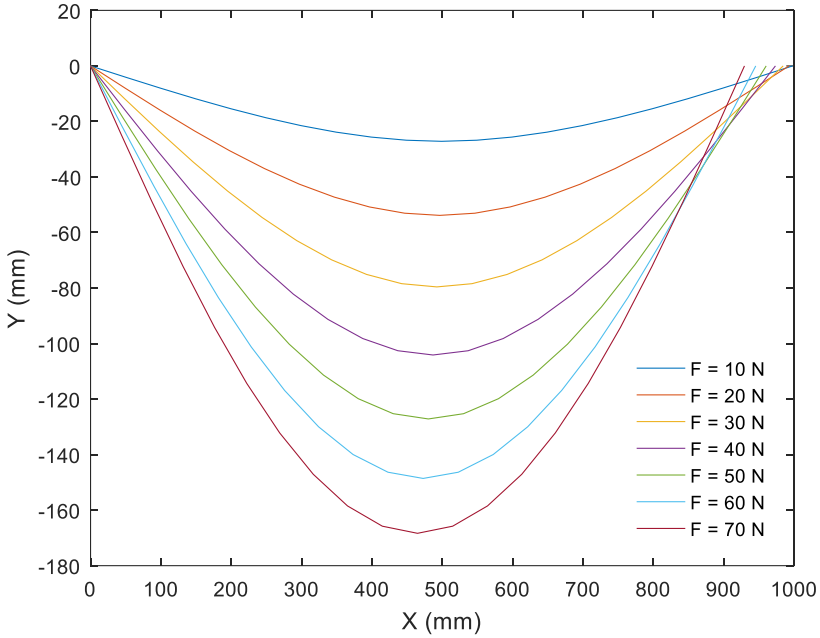

Figure 14 The deformed beam

The displacement vector of the midpoint after the deformation obtained from CBEM and MSC. ADAMS results are denoted by $\mathbf{d}_{\mathbf{CBEM}}$ and $\mathbf{d}_{\mathbf{ADAMS}}$ respectively. The difference percentage (DP) of the results are calculated as below

$$\mathrm{DP} = \frac{\|\mathbf{d}_{\mathbf{CBEM}}-\mathbf{d}_{\mathbf{ADAMS}}\|}{\min(\|\mathbf{d}_{\mathbf{CBEM}}\|,\|\mathbf{d}_{\mathbf{ADAMS}}\|)} \times 100 \tag{65}$$

Figure (15) shows the difference percentage of the results for different load magnitudes. According to this pic, DP is less than 0.09%, therefore, CBEM results are validated.

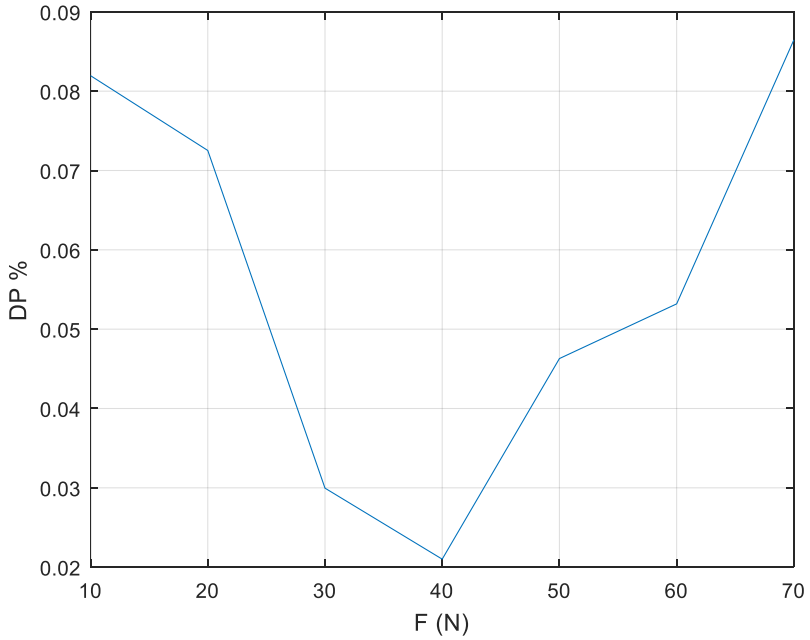

Figure 15 The difference percentage for different load magnitudes

9 Conclusions

In this paper, the CR formulation was studied for a planar beam with uniform cross-section which undergoes a large deformation. As shown in the paper, the method (CBEM) was explained thoroughly via simple mathematical relations that are used by engineers and students in the dynamics of multibody systems. This method is explained very straight forward and algorithmic via a planar cantilever beam as a case study which makes it easy to understand. In this case, the results were compared with the ones obtained by using the elliptic integrals. It is shown that the maximum relative error of results obtained by only three CR beam elements felt below 2%. Moreover the algorithm was generalized for 3D beams as well. At the end, a convergence study was conducted on the planar case. By investigating the results, it was seen that the results does not changed significantly when the number of elements becomes more than six elements. In addition, CBEM is implemented on a planar beam with simple- simple boundary conditions and the results showed satisfying accuracy which proves this method is very well suited for large deformation analysis of beams with uniform cross section.

References

[1] Bisshopp, K., and Drucker, D. C., "Large Deflection of Cantilever Beams", Quarterly of Applied Mathematics, Vol. 3, No. 3, pp. 272-275, (1945).

[2] Frisch-Fay, R., "*Flexible Bars*", Butterworths, London, (1962).

[3] Zhang, A., and Chen, G., "A Comprehensive Elliptic Integral Solution to the Large Deflection Problems of Thin Beams in Compliant Mechanisms", Journal of Mechanisms and Robotics, Vol. 5, No. 2, pp. 021006, (2013).

[4] Wang, C.M., and Kitipornchai, S., "Shooting Optimization Technique for Large Deflection Analysis of Structural Members", Engineering Structures, Vol. 14, No. 4, pp. 231-240, (1992).

[5] Pai, P.F., and Palazotto, A.N., "Large-deformation Analysis of Flexible Beams", International Journal of Solids and Structures, Vol. 33, No. 9, pp.1335-1353, (1996).

[6] Yin, X., Lee, K.M., and Lan, C.C., "Computational Models for Predicting the Deflected Shape of a Non-uniform, Flexible Finger", In Robotics and Automation, Proceedings, ICRA'04, 2004 IEEE International Conference, New Orleans, LA, USA, Vol. 3, pp. 2963-2968, (2004).

[7] Bathe, K.J., Ramm, E., and Wilson, E.L., "Finite Element Formulations for Large Deformation Dynamic Analysis", International Journal for Numerical Methods in Engineering, Vol. 9, No. 2, pp. 353-386, (1975).

[8] Bathe, K.J., and Bolourchi, S., "Large Displacement Analysis of Three-dimensional Beam Structures", International Journal for Numerical Methods in Engineering, Vol. 14, No. 7, pp. 961-986, (1979).

[9] Pai, P.F., Anderson, T.J., and Wheater, E.A., "Large-deformation Tests and Total-Lagrangian Finite-element Analyses of Flexible Beams", International Journal of Solids and Structures, Vol. 37, No. 21, pp. 2951-2980, (2000).

[10] Borri, M., and Merlini, T., "A Large Displacement Formulation for Anisotropic Beam Analysis", Meccanica, Vol. 21, No. 1, pp. 30-37, (1986).

[11] Urthaler, Y., and Reddy, J.N., "A Corotational Finite Element Formulation for the Analysis of Planar Beams", International Journal for Numerical Methods in Biomedical Engineering, Vol. 21, No. 10, pp. 553-570, (2005).

[12] Felippa, C.A., and Haugen, B., "A Unified Formulation of Small-strain Corotational Finite Elements: I. Theory", Computer Methods in Applied Mechanics and Engineering, Vol. 194, No. 21, pp. 2285-2335, (2005).

[13] Shabana, A.A., "*Dynamics of Multibody Systems*", Cambridge University Press, London, (2013).

[14] Shabana, A.A., "Definition of the Slopes and the Finite Element Absolute Nodal Coordinate Formulation", Multibody System Dynamics, Vol. 1, No. 3, pp. 339-348, (1997).

[15] Shabana, A.A., Hussien, H.A., and Escanola, J.L., "Application of the Absolute Nodal Coordinate Formulation to Large Rotation and Large Deformation Problems", Journal of Mechanical Design, Vol. 120, No. 2, pp. 188-195, (1998).

[16] Shabana, A.A., and Yakoub, R.Y., "Three Dimensional Absolute Nodal Coordinate Formulation for Beam Elements: Theory", Journal of Mechanical Design, Vol. 123, No. 4, pp. 606-613, (2001).

[17] Gerstmayr, J., Sugiyama, H., and Mikkola, A., "Review on the Absolute Nodal Coordinate Formulation for Large Deformation Analysis of Multibody Systems", Journal of Computational and Nonlinear Dynamics", Vol. 8, No. 3, pp. 031016, (2013).

[18] Fish, J., and Belytschko, T., "*A First Course in Finite Elements*", John Wiley and Sons, New York, (2007).

[19] Conn, Andrew R., Nicholas IM Gould, and Ph L. Toint, "Trust Region Methods", Vol. 1, Siam, (2000).

Nomenclature

A	Area of the cross section
DP	The difference percentage
e	The absolute error
e^*	The relative error
$\mathbf{e_z}$	The unit vector along the Z-axis
E	Young's modulus
$\mathbf{f_{ext}}$	The applied external force

$\mathbf{f_i}$	Nodal force
I	The second moment of area of the cross section
K	Stiffness matrix
l	Length of the element
L	Length of the beam
$\mathbf{M_{ext}}$	The applied external torque
$\mathbf{M_i}$	Nodal bending torque
$\mathbf{r_{end}}$	Position of the end point
$\mathbf{r_i}$	Position of the (i)th node in the (i-1)th frame
${}^{j}_{i}\mathbf{R}$	The rotation matrix from the (i)th to the (j)th frame
$\mathbf{W_i}$	Nodal wrench array
X_i, Y_i, Z_i	Axes of the (i)th frame

Greek symbols

$\delta_{x_i}, \delta_{y_i}, \delta_{z_i}$	The relative displacement of the (i)th node with respect to the (i-1)th node along the respective axis
$\delta\theta_{ix}, \delta\theta_{iy}, \delta\theta_{iz}$	The relative rotation of the cross section at the (i)th node with respect to the (i-1)th node along the respective axis
$\Delta_{\mathbf{end}}$	Deflection of the end point calculated by CBEM
$\Delta^{*}_{\mathbf{end}}$	Deflection of the end point calculated by elliptic integrals
$\Delta_{\mathbf{i}}$	The relative nodal deformation array

Appendix

In this section, the mathematical procedure is elaborated in order to implement CBEM on a planar beam with simple- simple boundary conditions under a vertical load at the middle and obtain the deflections. By using 20 elements, the (10)th node (N_{10}) is located at the middle of the beam and the load is applied on this node (Figure (16)). After the deformation, the angle of slope of the centroid curve is denoted by θ_0. In order to apply CBEM, the geometrical constraint at point B (N_{20}) is replaced by a constraint force, namely, C_y. Also the reference frame ($X^{'},Y^{'},Z^{'}$) is placed on point A, so that the X'-axis is tangent to the centroid curve of the deformed beam (Figure (17)).

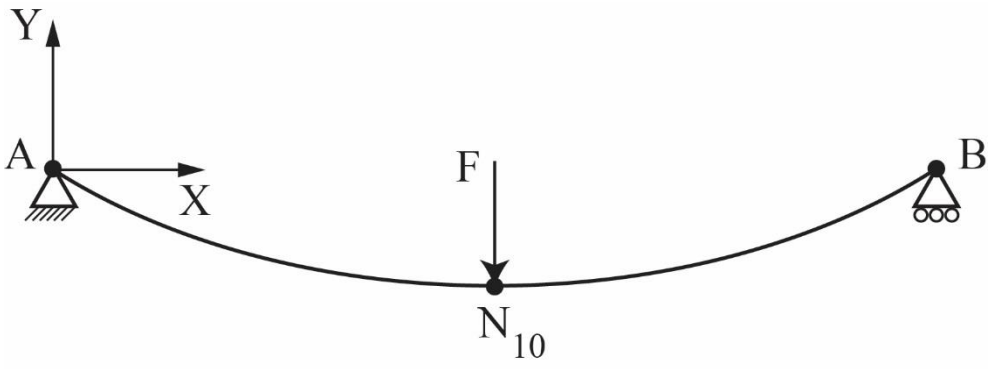

Figure 16 The beam after deformation

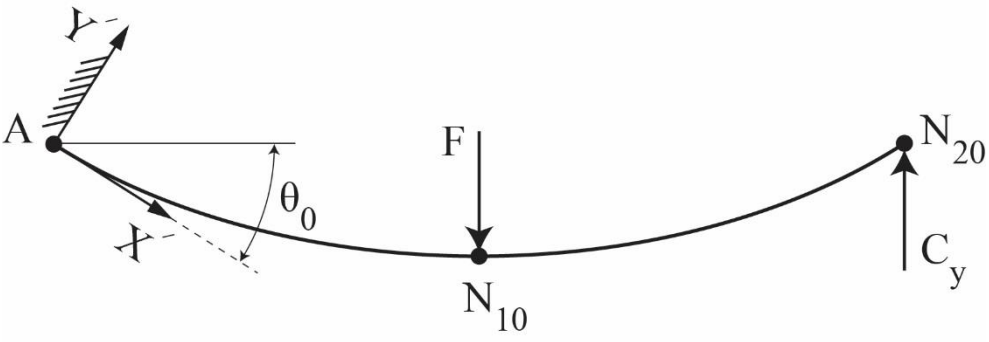

Figure 17 Some considerations

By taking the aforementioned considerations into account, the beam can be treated as a cantilever in the (X',Y',Z') reference frame and the formulation presented in section (5) can be easily implemented with some minor modifications, as the following.

The transformation matrix for (X,Y,Z) to (X',Y',Z') is denoted by $\mathbf{R}'$

$$\mathbf{R}'=\begin{bmatrix}\cos\theta_0 & \sin\theta_0\\ -\sin\theta_0 & \cos\theta_0\end{bmatrix} \qquad (A.1)$$

and the transform matrix from the (i)th frame to the (i-1)th frame is the same as Eq. (5)

$$\mathbf{i}_{\mathbf{i-1}}\mathbf{R}=\begin{bmatrix}\cos\delta\theta_i & \sin\delta\theta_i\\ -\sin\delta\theta_i & \cos\delta\theta_i\end{bmatrix} \qquad (A.2)$$

The position vector of the (i)th node in the (i-1)th frame is

$$\mathbf{r_i}=[l_e+\delta x_i \quad \delta y_i]^T \qquad (A.3)$$

And the position vector of the (i)th node in the (X,Y,Z) reference frame is

$$\mathbf{r_{N_i}}=\mathbf{r_{N_{i-1}}}+\left[\mathbf{R}'\right]^T\times\left(\prod_{k=1}^{i-1}\left[{}^{k}_{k-1}\mathbf{R}\right]^T\right)\mathbf{r_i}=[x_{N_i} \quad y_{N_i}]^T \qquad (A.4)$$

$$\mathbf{r_{N_1}}=\left[\mathbf{R}'\right]^T\times\mathbf{r_1}=[x_{N_1} \quad y_{N_1}]^T \qquad (A.5)$$

The applied external force is modified as below

$$\mathbf{f}^{\mathbf{i}}_{\mathbf{ext}}=\begin{cases}[0 \quad C_y-F]^T & 1<i<10\\ [0 \quad C_y]^T & 11<i<20\end{cases} \qquad (A.6)$$

and the external torque equals

$$\mathbf{M_{ext}}=0\ \mathbf{e}_z \qquad (A.7)$$

Then, the force vector on the (i)th node with respect to the (i-1)th frame is defined as following

$$\mathbf{f_1}=\mathbf{f}^{\mathbf{1}}_{\mathbf{ext}} \qquad (A.8)$$

$$\mathbf{f_i}=[\mathbf{R}']\times\left(\prod_{k=1}^{i-1}{}^{k}_{k-1}\mathbf{R}\right)\mathbf{f}^{\mathbf{i}}_{\mathbf{ext}} \quad , \quad i\neq1 \qquad (A.9)$$

Also, the torque applied on the (i)th node is calculated as

$$\mathbf{M_i}=m_{iz}=\{\mathbf{M_{i+1}}\}+\{\mathbf{r_i}\}\times\{\mathbf{f_i}\} \ , \ i\neq n \qquad (A.10)$$

$$\mathbf{M_n}=\mathbf{M_{ext}} \qquad (A.11)$$

Finally, the load vector on the (i)th node in the (i-1)th frame is cast in the following form,

$$\mathbf{W_i}=[f_i \quad m_{iz}]^T \qquad (A.12)$$

And the equilibrium equation can be presented

$$\mathbf{W_i}=\mathbf{K_i}\boldsymbol{\Delta_i} \qquad (A.13)$$

In which Δ_i is the deformation vector of the (i)th node in the (i-1)th frame, namely,

$$\Delta_i=[\delta x_i \quad \delta y_i \quad \delta\theta_i]^T \qquad (A.14)$$

and $\mathbf{K}_i$ is the stiffness matrix. The set of key equations for the (i)th element can be derived as:

$$\Delta_i=\mathbf{K_i^{-1}}\mathbf{W_i} \qquad (A.15)$$

As a result, a system of 60 nonlinear equations with 62 unknowns is obtained.

Due to defining two extra unknowns (θ_0 and C_y), two extra equations must be added to Eq. (A.15). For this purpose, the geometrical boundary conditions must be taken into account. Since the beam has simple- simple boundary conditions, the torque on point A is zero, therefore,

$$x_{N_{20}}C_y - x_{N_{10}}F=0 \qquad (A.16)$$

Also, the displacement of the point B (N_{20}) along Y-axis is zero which results in

$$y_{N_{20}}=0 \qquad (A.17)$$

Eq. (A.15), Eq. (A.16) and Eq. (A.17) together, form system of form a system of 62 equations with 62 unknowns which can be solved numerically.

چکیده

هدف از این مقاله، تبیین فرمولاسیونی جدید از نوع المان محدود همگرد برای تحلیل تیرهایی با سطح مقطع یکنواخت است. روش المان محدود همگرد، غالبا در تحلیل سازه‌هایی که دچار تغییر شکل بزرگ می‌شوند، مورد استفاده قرار می‌گیرد. در این پژوهش، المان‌های مورد نظر از فرضیات تیر اویلر- برنولی پیروی می‌کنند. برخلاف فرمولاسیون‌های ارائه شده در سایر مقالات، در این پژوهش از تعدادی مختصات نودی نسبی بهره‌گیری می‌شود که توصیف سینماتیکی تیر تغییر شکل یافته را بسیار آسان می‌کند، بدون آنکه نیازی به بیان روابط سینماتیکی پیچیده باشد. به منظور توضیح روش مورد نظر، فرمولاسیون ارائه شده، مرحله به مرحله بر روی یک تیر یکسرگیردار صفحه‌ای پیاده می‌شود. پس از مقایسه‌ی نتایج این روش با نتایج حاصل از حل تحلیلی (روش انتگرال‌های بیضوی)، مشاهده می‌شود که فرمولاسیون ارائه شده از دقت خوبی برخوردار است. در ادامه نیز به طور مختصر، فرمولاسیونی برای تیرهای فضایی ارائه می‌گردد.